



Dynamic Pore-Pressure Fluctuations in Rapidly Shearing Granular Materials

Richard M. Iverson; Richard G. LaHusen

Science, New Series, Vol. 246, No. 4931. (Nov. 10, 1989), pp. 796-799.

Stable URL:

<http://links.jstor.org/sici?sici=0036-8075%2819891110%293%3A246%3A4931%3C796%3ADPFIRS%3E2.0.CO%3B2-V>

Science is currently published by American Association for the Advancement of Science.

Your use of the JSTOR archive indicates your acceptance of JSTOR's Terms and Conditions of Use, available at <http://www.jstor.org/about/terms.html>. JSTOR's Terms and Conditions of Use provides, in part, that unless you have obtained prior permission, you may not download an entire issue of a journal or multiple copies of articles, and you may use content in the JSTOR archive only for your personal, non-commercial use.

Please contact the publisher regarding any further use of this work. Publisher contact information may be obtained at <http://www.jstor.org/journals/aaas.html>.

Each copy of any part of a JSTOR transmission must contain the same copyright notice that appears on the screen or printed page of such transmission.

JSTOR is an independent not-for-profit organization dedicated to and preserving a digital archive of scholarly journals. For more information regarding JSTOR, please contact support@jstor.org.

perature plots (12), as opposed to changes in the intercepts of such plots. These data are consistent with a change in the heat loss constant (Fig. 3), as opposed to an increase in the rate of power production by the electrolysis cell. Careful calibration of the rate of heat loss and accounting for all sources of additional heat generation (gas recombination and so forth) are required before one can unambiguously assign a change in temperature of the electrolysis cell to an unexplained chemical or nuclear power-producing process. If required, more accurate power production measurements on the Pd/D₂O/Pt system could only readily be made in closed-system calorimeters, where a well-defined heat path can be established and total recombination of the gases can be assured.

Note added in proof: In recent experiments in a closed-system calorimeter with total recombination of the gases, a recast Pd rod (0.39 cm in diameter and 1.0 cm in length) at 58 mA/cm² current density in 0.1M LiOD/D₂O produced no measurable excess power [$P_{\text{meas}} = (100 \pm 2\%)$ of P_{app}] for a period of over 12 days.

REFERENCES AND NOTES

1. M. Fleischmann, S. Pons, M. Hawkins, *J. Electroanal. Chem.* **261**, 301 (1989).
2. S. Gross, *Energy Convers.* **9**, 55 (1969).
3. A similar calculation has been independently performed: G. Kreysa, G. Marx, W. Plieth, *J. Electroanal. Chem.* **266**, 437 (1989). There are two errors in column c in table 2 of (1). The values for the rods of 0.2- and 0.4-cm diameter at 8 mA/cm² should be 143 and 306%, respectively.
4. J. M. Sherfey and A. Brenner, *J. Electrochem. Soc.* **105**, 665 (1958).
5. M. J. Joncich and N. Hackerman, *J. Phys. Chem.* **57**, 674 (1953).
6. R. G. Edkie and P. L. Khare, *Int. J. Heat Mass Transfer* **15**, 261 (1972).
7. S. C. Bhand *et al.*, *ibid.* **8**, 111 (1965).
8. W. E. Meyerhof, D. L. Huestis, D. C. Lorents, in preparation.
9. A. W. Szafranski and B. Baranowski, *J. Phys. E* **8**, 823 (1975).
10. R. Garwin, *Nature* **338**, 616 (1989).
11. N. S. Lewis *et al.*, paper presented at the Workshop on Cold Fusion Phenomena, 24 May 1989, Santa Fe, NM.
12. R. A. Huggins, *ibid.*
13. Supported by the Office of Naval Research and under a special grant from the California Institute of Technology. We thank G. Kreysa and W. Meyerhof for supplying preprints of related work. We thank C. A. Barnes and S. E. Kellogg for helpful criticism of this manuscript. Contribution 7969 from the Division of Chemistry and Chemical Engineering at the California Institute of Technology.

21 June 1989; accepted 29 August 1989

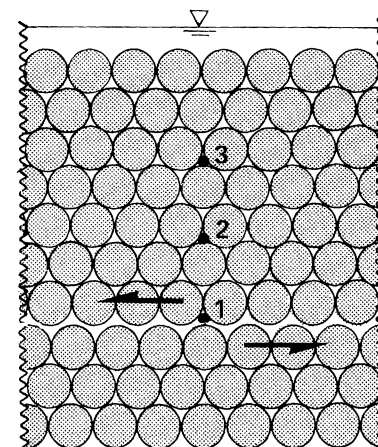


Fig. 1. Cross-sectional view through the center of the array of fiberglass rods. Water pressures were measured in individual pores indicated by numbered dots. Arrows show relative motion along the prescribed slip surface.

Dynamic Pore-Pressure Fluctuations in Rapidly Shearing Granular Materials

RICHARD M. IVERSON AND RICHARD G. LAHUSEN

Results from two types of experiments show that intergranular pore pressures fluctuated dynamically during rapid, steady shear deformation of water-saturated granular materials. During some fluctuations, the pore water locally supported all normal and shear stresses, while grain-contact stresses transiently fell to zero. Fluctuations also propagated outward from the shear zone; this process modifies grain-contact stresses in adjacent areas and potentially instigates shear-zone growth.

CLOSELY PACKED GRANULAR SOLIDS with interstitial pore spaces filled by liquid occur in both natural and man-made environments. Familiar examples include water-saturated soil and fragmented rock that compose most landslides, debris avalanches, and debris flows. Other examples include industrial slurries and granular mixtures, as well as saturated sediments that may be sheared during tectonic faulting.

Observations of mass-movement processes on the earth's surface have motivated fundamental questions about the dynamic role of pore water in rapidly sheared granular materials. For example, how can a water-

saturated mass of landslide debris liquefy and flow tens of kilometers across slopes as gentle as a few degrees—much farther than similar masses of dry debris and much farther than anticipated from the material's initial potential energy and coefficient of internal friction (1)? In most theories, liquefaction caused by high, quasi-static pore-water pressure gradients has been invoked to account for the mobility of wet rock debris (2), but high pore-pressure gradients are unlikely to persist in debris that flows steadily for minutes or even hours. Furthermore, water is an ineffective lubricant on most rock surfaces (3). Thus, pore water must enhance efficient, rapid shear deformation of rocky debris by some alternative means.

In this paper we describe experiments

testing a new hypothesis: that dynamic pore-pressure fluctuations can be generated as a result of grain rearrangements during rapid shear, and that the fluctuations can be large enough to modify grain-contact stresses significantly and promote efficient deformation. Specifically, transient increases in pore pressure in discrete domains where the granular phase momentarily contracts would inhibit further contraction and ease local shear displacement. Conversely, where the granular phase dilates, transient reduction in pore pressure would suppress further dilation and inhibit local shear displacement. In a deformation field in which local dilations and contractions accompany global shear, pore-pressure fluctuations may reduce frictional energy dissipation because they help localize intergranular shearing in areas of low or zero grain-contact stress (4). Such effects are enhanced if the pore fluid (for example, water) is relatively incompressible. An important lemma is that local dilation and contraction can occur even while the bulk deformation is steady (5, 6).

The tendency for pore-pressure fluctuations to develop during steady shear deformation depends on the relative rates of grain rearrangement and pore-pressure equilibration, which can be expressed by a single dimensionless parameter, $R = kE/\nu\mu\delta$ (7, 8) where k is the hydraulic permeability, E is the uniaxial (Young's) compression modulus of the composite granular medium, ν is the velocity of intergranular sliding, μ is the viscosity of the pore fluid, and δ is a characteristic length, typically the grain diameter. Within R the quantity kE/μ functions as a pore-pressure diffusivity, and $\delta^2\mu/kE$ is the time scale for diffusive pore-pressure equilibration over the distance δ . The quantity δ/ν is the time scale for pore dilation and contraction and thus for generation of pore-

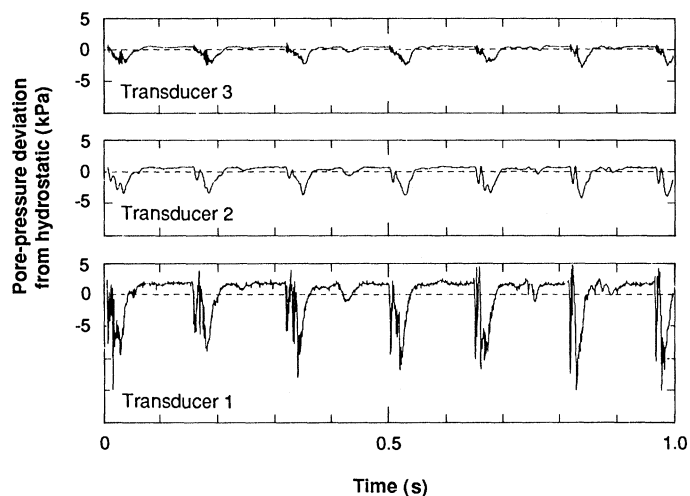
U.S. Geological Survey, Cascades Volcano Observatory, 5400 MacArthur Boulevard, Vancouver, WA 97661.

pressure fluctuations. R represents the ratio of these two time scales. Consequently, if R is large, transient pore-pressure disequilibrium across the distance δ tends to dissipate more rapidly than it is generated, and significant pressure fluctuations are unlikely to arise. If R is small, there is insufficient time for pore pressures to equilibrate as contraction or dilation occurs, and the potential for local pore-pressure fluctuations is enhanced. "Small" and "large" values of R correspond qualitatively to "rapid" and "slow" deformation, but experimentation is needed to give quantitative meaning to these qualitative descriptors.

To test our hypothesis we first conducted experiments in which R ranged between 10 and 50 and the mechanism producing pore-pressure fluctuations was regularly cyclic and easily understood. In these experiments, we measured fluctuations generated along a single slip surface in an idealized granular medium: a water-saturated, close-packed array of cylindrical fiberglass rods, each 290 mm in length, 19 mm in diameter, and spaced 0.12 mm from its neighbors (Fig. 1). The rod spacing and array geometry were fixed; neighboring rods were connected at their ends with polyethylene glue, except along the prescribed slip surface. After submersing the array in water, we withdrew trapped air from the pores between the rods using a vacuum pump and syringe. Aside from its regular geometry and packing, important physical properties of the water-submersed array (Table 1) matched those of typical landslide or debris-flow rubble.

Using a motor and pulley system, we sheared the array at steady speeds of 0.1 to 0.4 m s⁻¹. As shearing proceeded, the periodic bumpiness of the slip surface caused cyclic vertical motion of the rods, which in turn caused pore-volume changes and wa-

Fig. 2. Unfiltered time series of pore-water pressures measured at the locations marked in Fig. 1 during an experiment with a slip rate of 0.118 m s⁻¹. Dashed lines show hydrostatic reference pressures; 1 kPa is equivalent to the hydrostatic pressure at the base of a column of water about 0.1 m in height.



ter-pressure fluctuations along the slip surface. We sampled the water pressures at a frequency of 2750 Hz with miniature transducers positioned near the center of selected pores (Fig. 1).

Measured pore-pressure fluctuations exhibited a repetitive time-series pattern in which high-pressure plateaus were separated by deep, low-pressure troughs (Fig. 2). High-speed photographs show that the plateaus occurred when rods above the slip surface lost contact with the underlying rods and glided on a cushion of water. At such times the rods along the slip surface supported no normal or shear stress, and the weight of the rod array was supported entirely by the pore-pressure gradient between the slip surface and the top of the array. Low-pressure troughs occurred when the upper rods recontacted the underlying rods and then slid over them; this motion caused the intervening pores to dilate (9).

The dominant mode of the pore-pressure fluctuations was imperfectly periodic, despite the periodic slip-surface geometry and

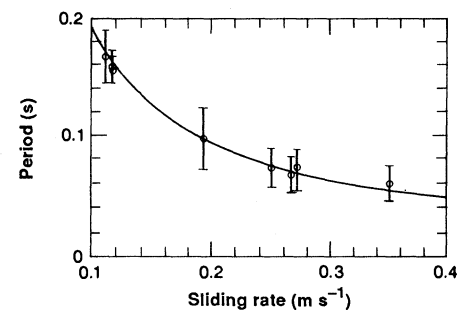


Fig. 3. Mean period of the dominant mode of pore-pressure fluctuation as a function of sliding rate for eight rod experiments. Error bars show ± 1 SD about the mean for each experiment. The curve shows theoretical periods computed for known sliding rates and rod diameters.

constant sliding rates. Apparently, slight inconsistencies in frictional and collisional rod interactions caused the dominant fluctuation periods to vary about the predicted mean (Fig. 3) and produced noisy power spectra and imperfect replicability.

Comparison of pore-pressure time series measured along the slip surface with those measured in the rod array shows that the pressure fluctuations propagated from their source at a subsonic speed (10) and simultaneously underwent frequency-dependent amplitude attenuation (Figs. 2 and 4). The low-frequency components of the fluctuations retained most of their power, however, and affected solid-contact stresses significantly when they arrived at points a few rod diameters distant (Fig. 4).

In a second set of experiments, we tested whether analogous pore-pressure fluctuations would arise during rapid shear deformation of realistic geological materials. Using facilities at the Japanese National Research Center for Disaster Prevention (NRCDP), we measured pore-water pressures in three artificial landslides composed of poorly sorted, sandy soil (Table 1) as they began to deform and mobilize into debris

Table 1. Static physical properties of experimental media.

Parameter	Fiberglass rod array	Artificial landslides
Grain properties		
Median diameter, δ	1.9×10^{-2} m	1.1×10^{-3} m
Trask size sorting coefficient	1.0	2.3
Specific gravity	2.3	2.6
Young's compression modulus	1.3×10^9 Pa	
Pore-water properties		
Specific gravity	1.0	1.0
Viscosity, μ	1.1×10^{-3} kg m ⁻¹ s ⁻¹	1.1×10^{-3} kg m ⁻¹ s ⁻¹
Bulk composite properties		
Vertical thickness	0.12 m	1.0 m
Porosity	0.10	0.48, 0.41*
Permeability, k	1.8×10^{-11} m ²	5.1×10^{-11} m ²
Young's compression modulus, E	5.1×10^6 Pa	6.0×10^6 Pa†
Coefficient of friction‡	0.45	0.54

*The two porosities are mean values measured before and after landsliding occurred. During sliding the soil underwent net contraction. †Measured quasistatically at 13 kPa confining pressure. ‡Measured in terms of effective stress, includes interlocking as well as intrinsic friction.

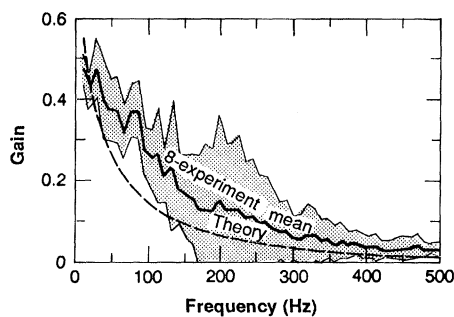


Fig. 4. Attenuation of amplitudes of pore-pressure fluctuations as a function of frequency for signal propagation from the slip surface. Gain reflects the ratio of the amplitude at transducer 2 to the amplitude at transducer 1 of Fig. 1. The heavy line and shaded region show the mean ± 1 SD for the eight experiments of Fig. 3. The dashed curve shows theoretical attenuation based on a simple pore-pressure diffusion model (8).

flows (11). We triggered the landslides by applying artificial rainfall and ground water to rectangular soil prisms that were 10 m long, 4 m wide, 1 m thick, and resting on a roughened, 30° concrete slope.

In each landslide experiment, we positioned three or four nests of pore-pressure transducers at 2-m intervals along the longitudinal axis of the soil prism, with individual transducers at depths of 0.5, 0.7, and 0.9 m measured normal to the slope. The transducers had screened diaphragm ports 4 mm in diameter, and all were below the water table when slope failure occurred. While each transducer output was sampled at 973 Hz, we measured surface displacement with extensometers and subsurface displacement of the slope with strain-gage wands (12).

Landslide displacement data indicate that slow premonitory downslope creep was concentrated in a shear zone at 0.8 to 0.95 m depth. Pore pressures did not respond to the premonitory creep until the final few seconds before failure, when downslope movement measured at the surface increased smoothly and rapidly from a rate of less than 0.001 m s^{-1} to a steady rate of about 1 m s^{-1} . During the period of rapid acceleration, pore pressures at 0.9 m depth initially declined, apparently as a result of soil dilation in the shear zone. Then, as the downslope velocity became steady, pore pressures in and adjacent to the shear zone rose sharply and began to fluctuate (Fig. 5). Although the details of the fluctuations differed for each transducer nest and each experiment, characteristic amplitudes and frequencies were remarkably consistent.

Comparison of pore-pressure fluctuations in the artificial landslides with those in the fiberglass rod experiments reveals both similarities and differences (9). For example, fluctuation amplitudes in the landslides were sufficiently large that vertical pore-pressure

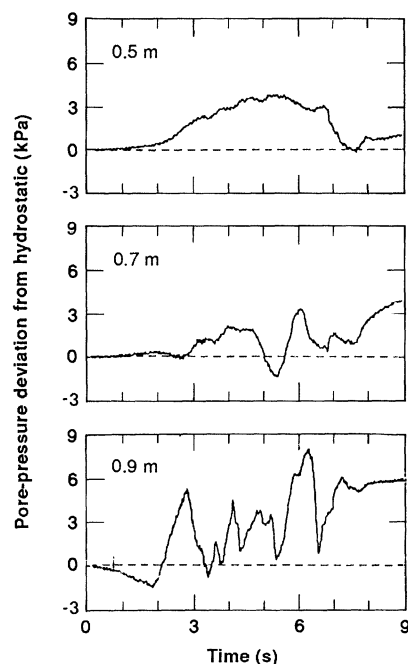


Fig. 5. Unfiltered time series of pore-water pressures measured at three depths during movement of artificial landslide. The time series began when landslide movement exceeded about 1 mm s^{-1} . Most landslide movement ceased after about 8 s. Dotted lines show hydrostatic reference pressures.

gradients transiently supported the entire overburden weight and locally reduced grain-contact stresses to zero. Furthermore, amplitudes of the fluctuations attenuated with distance from the shear zone. The dominant fluctuation frequency in the landslides, about 1 Hz, was much lower than in the rod arrays, however (compare Figs. 2 and 5). The low frequency of the fluctuations in the landslides probably reflects a phenomenon other than grain-by-grain rearrangement, because the relatively large transducer ports sampled pressures over tens of individual pores.

We conjecture that the low-frequency pressure fluctuations in the landslides may have resulted from the interaction of macroscopic blocks of soil that moved as nearly coherent units (13). If the size of such blocks scales with the landslide thickness (1 m), the landslide movement rate of 1 m s^{-1} might, by analogy to the rod experiments, produce pressure fluctuations with the observed dominant frequency, about 1 Hz (Fig. 5). Moreover, for $\delta = 1 \text{ m}$ and $\nu = 1 \text{ m s}^{-1}$, $R = 0.3$, a value that is much smaller than those of the rod experiments and therefore characteristic of conditions conducive to pressure fluctuations.

Alternatively, the landslide pore-pressure fluctuations may have resulted from systematic soil dilation and contraction that accompanied shear along a wavy basal surface (14).

We did not observe such a surface at the conclusion of any experiment, but we cannot rule out the possibility that one was present.

Confirmation of dynamic pore-pressure fluctuations in rapid landslides also motivates a further conjecture. Fluctuations that propagate from a localized shear zone may instigate deformation in adjacent zones by transiently reducing grain-contact stresses. The initial fluctuations may thus catalyze further fluctuations, and this positive feedback may transform the deformation style from slide to flow.

REFERENCES AND NOTES

1. A. M. Johnson, in *Slope Instability*, D. Brunsten and D. B. Prior, Eds. (Wiley, New York, 1984), pp. 257–361; K. Sassa [*Jpn. Minist. Educ. Sci. Cult. Proj. Rep. 61480062* (1988)] reported data that clearly differentiate the efficiencies of wet and dry rocky flows.
2. Soil liquefaction and flow caused by a quasi-static pore-pressure field is similar to fluidization of particulate beds and requires an upward pore-pressure gradient that balances the force due to gravity [A. Casagrande, *Harv. Soil Mech. Ser.* **88**, 1 (1976); R. M. Iverson and J. J. Major, *Water Resour. Res.* **22**, 1543 (1986)]. If no fluid enters the base of the liquefied mass, such an upward gradient can be maintained only while there is net settling or contraction of the granular phase with concomitant displacement of pore water [compare K. Sassa, *Proceedings of the IVth International Symposium on Landslides, Toronto* (1984), vol. 2, p. 349; J. N. Hutchinson, *Can. Geotech. J.* **23**, 115 (1986)], a process that cannot persist during steady flow.
3. J. K. Mitchell, *Fundamentals of Soil Behavior* (Wiley, New York, 1976).
4. A similar mechanism, acoustic fluidization, might operate in the absence of pore-pressure effects if strong acoustic vibrations are transmitted across intermittent grain contacts [H. J. Melosh, *J. Geophys. Res.* **84**, 7513 (1979)]. However, the presence of a continuous interstitial liquid greatly facilitates the process by providing a medium that sustains and transmits local pressure imbalances until pressures equilibrate through fluid flow.
5. T. G. Drake and R. L. Shreve, *J. Rheol.* **30**, 981 (1986).
6. O. R. Walton and R. L. Braun, *ibid.*, p. 949.
7. J. W. Rudnicki, *J. Geophys. Res.* **89**, 9259 (1984).
8. R. M. Iverson, *Abstracts of the 28th International Geological Congress*, 9 to 19 July 1989, Washington, DC (International Geologic Congress, Washington, DC, 1989), vol. 2, pp. 104–105.
9. In the rod experiments, the time-averaged mean pore pressures differed insignificantly from the static pressures recorded before shearing. In the landslide experiments, the time-averaged mean pore pressures were greater than the original static pressures, as a result of bulk contraction of the landslide mass.
10. Inferred wave speeds were somewhat greater than those predicted for the slow, diffusive mode by the poroelastic theory of M. A. Biot [*J. Acoust. Soc. Am.* **28**, 168 (1956)], but were much less than those predicted for the fast compressive mode.
11. The soil was granite grus from Mount Tsukuba, Japan.
12. Experimental design and measurement procedures, with the exception of those used to make high-frequency pore-pressure measurements, were developed by T. Fukuzono [*Proceedings of the IVth International Conference and Field Workshop on Landslides, Tokyo*, 3 to 9 September 1985, p. 145].
13. J. Lee, S. C. Cowin, J. S. Templeton [*Trans. Soc. Rheol.* **18**, 247 (1974)] documented movement of grains in coherent clusters or blocks during flow in hoppers, and Drake and Shreve (5) documented the same effect during rapid open-channel flow.
14. R. L. Baum and A. M. Johnson, *U.S. Geol. Surv.*

Bull. 1842, in press.

15. We thank C. Davis and E. Harrison for their assistance with data collection and analysis. E. Harp and J. Walder provided thoughtful critiques for the manuscript. The NRCDD rainfall and landslide simulator was used with the help and collaboration of T. Fukuzono, M. Tominaga, H. Moriwaki and N.

Oyagi, as part of the NRCDD project on snow avalanche management and landslide prediction and control. Our work was supported by a United States-Japan cooperative program on research and development in science and technology.

29 August 1989; accepted 26 September 1989

Germ-Line Transmission of a *c-abl* Mutation Produced by Targeted Gene Disruption in ES Cells

PAMELA L. SCHWARTZBERG, STEPHEN P. GOFF, ELIZABETH J. ROBERTSON

A substitution mutation has been introduced into the *c-abl* locus of murine embryonic stem cells by homologous recombination between exogenously added DNA and the endogenous gene, and these cells have been used to generate chimeric mice. It is shown that the *c-abl* mutation was transmitted to progeny by several male chimeras. This work demonstrates the feasibility of germ-line transmission of a mutation introduced into a nonselectable autosomal gene by homologous recombination.

THE INTRODUCTION OF MUTATIONS into the germ line of an organism is one of the most powerful genetic methods for determining the functions of a specific gene product (1). Recent advances in the detection of rare homologous recombination events have facilitated the modification of defined chromosomal loci in mammalian cell lines (2-8). The use of these techniques in combination with cultured embryonic stem (ES) cells should now allow the replacement of normal cellular genes in the mouse germ line by mutant alleles with defined sequence alterations (9). ES cells are pluripotent cells derived from preimplantation mouse embryos (10), which can be propagated in culture and subsequently re-introduced into mouse blastocysts by microinjection to form chimeric mice. Such chimeras, if constructed with euploid ES cells, have high rates of transmission of the ES cell component in the germ line (11). To date, however, only mutations at the X-linked locus encoding the enzyme hypoxanthine-guanine phosphoribosyl transferase (HGPRT), for which there are genetic selections, have been successfully transferred into the mouse germ line by this strategy (12, 13).

We are interested in the function of *v-abl*, the oncogene carried by the Abelson murine leukemia virus (A-MuLV), and its cellular homolog *c-abl* (14). A-MuLV causes the

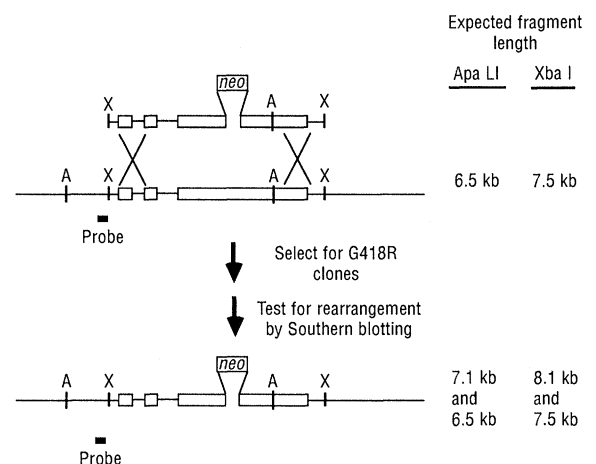
rapid induction of lymphosarcoma in susceptible mice and can transform both fibroblasts and lymphocytes in culture (15, 16). The human *c-abl* has been implicated in at least two forms of cancer, chronic myelogenous leukemia and acute lymphocytic leukemia, where the gene is activated by chromosomal translocation (17). Although much is known about the oncogenic potential of both *v-abl* and *c-abl*, little is known about the function of the normal gene in development or in the life of the adult organism. The *c-abl* gene is transcribed in most tissues to give rise to at least two major mRNAs found in approximately equal abundance (18). Post-meiotic spermatids have been shown to express very high levels of a distinctive *c-abl* mRNA (19, 20) that is truncated in the 3' untranslated region by polyadenylation at a novel site (21). The roles of the *c-abl* protein (Abl) in these cells and in the rest of the organism remain obscure, although its

membership in the class of tyrosine-specific kinases suggests that it may be involved in signal transduction. The generation of defined mutations in *c-abl* in the mammalian germ line could provide insights into the function of the gene product.

We have used homologous recombination to introduce a substitution mutation into the *c-abl* locus of mouse ES cells. We chose to introduce mutations affecting only the COOH-terminal third of the Abl protein, downstream from the tyrosine kinase domain and nuclear targeting sequences (22). Since *c-abl* is expressed ubiquitously, we were concerned that introduction of a null mutation would have severe deleterious effects on the development of the mouse, or might even be lethal, at a very early stage. Mutations limited to this region might not represent null mutations and might generate a less severe phenotype. Deletions affecting the COOH-terminus of *v-abl* have shown that this domain is not needed for tyrosine kinase activity or for the transformation of fibroblasts but is important for transformation of lymphocytes. These deletion mutants also exhibit a reduction in the toxicity associated with high-level expression of the wild-type viral oncogene in certain cell lines (23). The tissue specificity of the effects of these mutations in A-MuLV suggested that we might obtain informative tissue-specific phenotypes from similar mutations in *c-abl*.

To select for the rare homologous recombination of DNA with the endogenous *c-abl* locus, we designed a DNA construct, pAbXR1, in which a promoterless neomycin-resistance gene (*neo^r*) is fused to *c-abl* genomic sequences (24); this DNA would confer resistance to the drug G418 only after certain recombination events. Expression of *neo* in the construct could be activated either when a nonhomologous integration event places the sequence next to an arbitrary cellular promoter, or, alternatively, when homologous recombination inserts

Fig. 1. Scheme for the replacement of the normal *c-abl* gene with a *c-abl-neo* fusion by homologous recombination. A linear DNA containing *neo* embedded in *c-abl* sequences, but devoid of signals for transcription and translation, is introduced by electroporation (27). A double crossover in the flanking *c-abl* sequences replaces the normal gene with the fusion gene and activates expression of the *neo*. After digestion of DNA from drug-resistant clones with *Apa* I and *Xba* I, hybridization with the flanking probe EX (28) detects DNA fragments of novel sizes from the mutant allele, as well as fragments of the normal size from the unaltered allele. A, *Apa* I; X, *Xba* I.



P. L. Schwartzberg and S. P. Goff, Department of Biochemistry and Molecular Biophysics, Columbia University, College of Physicians & Surgeons, New York, NY 10032.

E. J. Robertson, Department of Genetics and Development, Columbia University, College of Physicians & Surgeons, New York, NY 10032.